KSME International Journal, Vol. 17 No. 10, pp. 1543~1551, 2003

Direct Numerical Simulation of Channel Flow with Wall Injection

Yang Na*
Multidisciplinary Aerospace System Design Team
Department of Mechanical Engineering, Konkuk University,
Hwayang-dong 1, Gwangjin-gu, Seoul 143-701, Korea

The present study investigates turbulent flows subject to strong wall injection in a channel through a Direct Numerical Simulation technique. These flows are pertinent to internal flows inside the hybrid rocket motors. A simplified model problem where a regression process at the wall is idealized by the wall blowing has been studied to gain a better understanding of how the near-wall turbulent structures are modified. As the strength of wall blowing increases, the turbulence intensities and Reynolds shear stress increase rapidly and this is thought to result from the shear instability induced by the injected flows at the wall. Also, turbulent viscosity grows rapidly as the flow moves downstream. Thus, the effect of wall-blowing modifies the state of turbulence significantly and more sophisticated turbulence modeling would be required to predict this type of flows accurately.

Key Words: Turbulent Flow, Wall Injection, Direct Numerical Simulation, Turbulent Viscosity

Nomenclature

c_f : Skin friction coefficient based on inlet bulk velocity
h : Half channel height
L_x, L_z : Domain size in the streamwise and spanwise directions, respectively.
p : Pressure
t : Time
Re_h : Reynolds number based on inlet bulk velocity, $U_b h/\nu$
$\mathrm{Re}_{u'v'}$: $-\dfrac{\overline{u'v'}}{u_{rms}v_{rms}}$
Re_τ : Reynolds number based on inlet friction velocity, $u_{\tau,inlet}h/\nu$
U_b : Bulk velocity at inlet of the computational domain
U_c : Convection velocity
U_{mean} : Averaged streamwise velocity
U^+ : Mean streamwise velocity made dimensionless with inlet friction velocity
u_i : Velocity component, $i=1, 2, 3$
u_{rms}, v_{rms}, w_{rms} : Turbulence intensities in x, y and z directions.
u_τ : Friction velocity
x, y, z : Cartesian coordinate in the streamwise, wall-normal and spanwise directions

Greek Letters

ε : Wall injection parameter, V_w/U_b
ν_t : Turbulent viscosity

* **E-mail** : yangna@konkuk.ac.kr
TEL : +82-2-450-3467; **FAX** : +82-2-447-5886
Multidisciplinary Aerospace System Design Team, Department of Mechanical Engineering, Konkuk University, Hwayang-dong 1, Gwangjin-gu, Seoul 143-701, Korea. (Manuscript **Received** December 30, 2002; **Revised** July 3, 2003)

1. Introduction

Turbulence plays an important role in the evolution of internal flow of hybrid rocket motor from a fluid mechanics point of view. Since the near-wall state of turbulence is likely to be modified due to the effect of wall blowing, caution needs to be made when the RANS type calcula-

tions are to be performed. In addition to the usual effect of turbulence on the flow, there are several complications involving the turbulence that should be considered in order to enhance the overall rocket performance. For example, turbulence interacts with combustion process through the pressure and turbulent fluctuations and this would in turn influence on the dispersion process of boron or aluminum oxide particles. Also turbulence will be driven by fluctuations created in the combustion layer and flow instability may develop under a certain operational condition.

Better understanding of these injection driven flows such as those present in hybrid rocket motors would require the high quality data on the statistics and turbulence mechanisms but there has been significantly less effort both in experimental and turbulence modeling studies than in other common shear flows. Most of previous studies (Williams et al., 1969 ; Beddini, 1986 ; Traineau et al., 1986 ; Dunlap et al., 1990 ; Liou and Lien, 1995) devoted to the analysis of wall-bounded flows with wall injection have dealt with very weak blowing. Consequently a success would be limited if the results of those works are used for the design of the flows with strong wall injection. This fact is reflected by a difficulty of predicting the flows using currently available turbulence models with satisfactory accuracy. The present work is motivated by the need for the data of turbulent flows with strong wall-injection to understand the physical process in near-wall region and to support the turbulence and LES modeling developments. Thus, a method of direct numerical simulation is used for the present study and the results are presented for the mean flow and turbulence quantities.

2. Numerical Methodology

2.1 Governing equations

A simplified model has been considered to enable DNS and the schematic diagram of three-dimensional computational domain is shown in Fig. 1. In this type of turbulent flows, both surface curvature and wall injection influences the evolution of the core flow but in order to isolate the effect of wall blowing only, flat plate walls were considered. The streamwise extent of the domain is $L_x=26h$, the spanwise extent is $L_z=6.5h$ where h is the half channel height. The choice of the domain size is based on the two point correlation data of several previous DNS studies conducted for the simple channel flows (Kasagi and Shikazono, 1995 ; Kim et al., 1987 ; Na et al., 1999). In terms of wall units (based the wall friction velocity at the inlet of the domain), the domain size is roughly equivalent to 3820, 294, 955 in the streamwise, wall-normal and spanwise directions, respectively and about 1900 wall units are allowed for the injection-driven flow regime. By referencing to most of the available DNS results, the it is thought that about 1900 wall unit is generally all right to capture the characteristics of the turbulent flow. Obviously, a larger domain size in the streamwise direction would be helpful in scrutinizing the long-time evolution of the injection-driven flow but the main purpose of the paper is to investigate how the turbulence is modified by the streamwise acceleration induced by strong injection. Thus it was thought that the current domain size serves to our aim reasonably (even if not perfectly) well and it was decided that the more information of the flow which will be only available from the simulation with a longer domain size would not be worth of a large increase of computational cost at the moment. Thus, any attempt of increasing the domain size was not made at the present time. The Reynolds number based on inlet bulk velocity and a half channel height, Re_h, is 2250.

The strength of wall-injection is denoted by

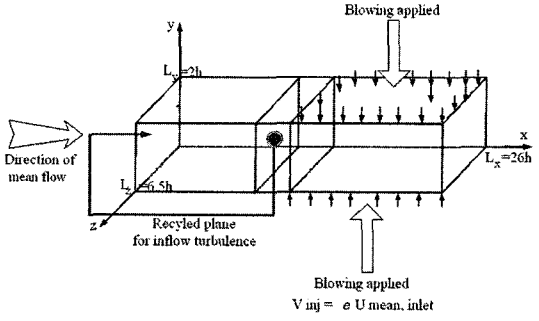

Fig. 1 Flow configuration

$\varepsilon = V_w / U_b$ where V_w is the applied wall normal velocity at the wall and U_b is the bulk velocity at inlet of the domain. Wall injection starts from $x/h=13.4$ along the both upper and lower walls.

Since the Mach number in the hybrid motor is in general less than 0.1, following non-dimensionalized governing equations for velocity field of unsteady incompressible viscous flows are solved on a rectangular staggered grid (Harlow and Welch, 1965).

$$\frac{\partial u_i^*}{\partial x_i^*}=0 \tag{1}$$

$$\frac{\partial u_i^*}{\partial t^*}+\frac{\partial}{\partial x_j^*}(u_i^* u_j^*)=-\frac{\partial p^*}{\partial x_i^*}+\frac{1}{Re_h}\frac{\partial^2 u_i^*}{\partial x_j^* x_j^*} \tag{2}$$

All the variables are made dimensionless using an inlet bulk velocity and a half-channel height and the superscript $*$ will be dropped hereinafter for convenience.

The governing equations (1)-(2) are integrated in time using a semi-implicit scheme. A low-storage three-substep, third order Runge-Kutta scheme (Spalart et al., 1991) is used for treating convective terms explicitly and a second order Crank-Nicolson scheme is used for treating viscous terms implicitly. All spatial derivatives are approximated with second order central difference scheme.

2.2 Boundary conditions

The no-slip boundary is used along the wall except in a region where constant blowing is applied ($x/h>13.4$). The flow is assumed to be homogeneous in the spanwise direction, justifying the use of periodic boundary conditions in that direction.

The outflow boundary condition is the following widely-used convection boundary condition, which is believed to allow the turbulent structures generated inside the domain to leave smoothly.

$$\frac{\partial u_i}{\partial t}+U_c\frac{\partial u_i}{\partial x}=0 \tag{3}$$

where U_c is the convection velocity. In order to see how the exit boundary condition disturbs the flow in the vicinity of the exit, a time sequence of vertical velocity (which is believed to be very sensitive to the exit boundary condition) contours has been analyzed and it has been found that those structures leave the exit domain rather smoothly. Of course, this one result can not tell that the distortion associated with the convective boundary condition is not present but it rather implies that the convective boundary condition can be a reasonable candidate for this type of flow. However, the caution should be made when analyzing the flow close to the exit due to the possible contamination and thus, any analysis was avoided in a region in the vicinity of exit.

In order to generate inflow turbulence as a function of time, a part of periodic channel is attached in front of the domain of main interest but any attempt to re-scale the flow field using a method of Lund et al.(1998) was not made since the streamwise acceleration of the flow results in non-negligible inhomogeneity in the presence of strong wall blowing. The 'recycled' plane should be located as far upstream as possible from a region of injection in order to be free from the influence of 'injection-driven' flow. At the same time, this plane should be located as far downstream as possible from the inlet so that the two planes are not correlated to avoid periodicity. Thus there must be a compromise between the quality of inlet condition and the cost of the computation. The 'recycling' location of $x/h=12$ was chosen, through several iterations, to meet the both requirements mentioned above: (1) The plane at $x/h=12$ is about 1700 wall units apart from the inlet and this ensures the zero-correlation, (2) Also, the statistics calculated at this location is undistinguishable from those obtained between $x/h=0$ to 12. This indicates that the recycled plane represents the correct turbulent state of the simple channel flow, which is what we design to achieve, and is not influenced by the presence of injection which starts from $x/h=13.4$.

2.3 Computational details

Two different cases were studied. For Case-1, ε is set to 0.01 and for Case-2, to 0.05. Depending on the strength of wall injection, two different

resolutions were used for the simulations. The Case-1 was analyzed on $257\times129\times129$ grids and the Case-2 was on $513\times257\times129$ grids. The Reynolds number, $U_b h/\nu$ is 2250 for both cases and it is approximately equivalent to $Re_\tau\approx150$ if the inlet friction velocity is used.

Based on the inlet friction velocity, the grid spacing for both Case-1 in the streamwise direction is $\Delta x^+\approx15.3$ in wall units. In the wall normal direction, the minimum grid spacing is $\Delta y^+_{\min}\approx 0.023$ at the wall and the maximum grid spacing isin the middle of the channel. In the spanwise direction, grid spacing is $\Delta z^+_{\min}\approx7.7$. For Case-2, a higher resolution is adopted to capture the shear layer more accurately due to the increased complexity in the flow by strong wall injection. In order to see the effects of resolution, three different grid systems were tested ($257\times129\times129$, $257\times127\times129$, $513\times127\times129$) and it was found that the resolution in the vertical direction does not make significant changes to the first-order statistics and the resolution in the streamwise direction is more important than in the vertical direction. The $513\times257\times129$ grid system gives the grid resolution of approximately $\Delta x^+\approx7.5$, $\Delta y^+_{\min}\approx0.0055$, $\Delta y^+_{\max}\approx1.8$, $\Delta z^+\approx7.5$. Compared to the previous work on channel flow by spectral method by Na et al.(1999) and Miyauchi and Tanahashi's turbulent mixing layer simulation (1993), the resolution chosen in the present study is much better in both of regions with and without wall-injection. Many statistical quantities in the region without wall injection ($x/h<13.4$) agree with those of Kasagi and Shikazono (1995) and Na et al. (1999). However, if one is interested in higher order statistics or any quantities which are very sensitive to small scales, say, energy spectra in a high wave number region, one should resort to higher resolution in order to obtain accurate results not contaminated by the truncation error of second order central difference.

For the calculation of statistical quantities, averages were performed over the homogeneous spanwise direction and time and hence, single-point statistics are functions of both x and y. In the present study, the flow experiences complex changes after the injection is applied and this causes slower statistical convergence than in the upstream. The total averaging time was 120 h/U_b for Case-1 and 60 h/U_b for Case-2. This is equivalent to about 9.2 and 4.6 flow-through times if the flow-through time is defined as the full trip time of fluid particles through a region of wall-injection.

3. Results

Since the strength of wall injection is 5 times higher for Case-2, the flow experiences stronger streamwise acceleration or inhomogeneity for the latter case. Even though the effect of wall injection is more pronounced in the latter case, the results indicate that two cases show very similar characteristics of injection-driven flow. Thus, in order to create a better focus, the results from the Case-2 will be presented hereinafter.

Figure 2 shows instantaneous streamwise velocity contours in the $(x-y)$ plane in the middle of the spanwise domain for Case-2. The first figure shows the flow characteristics upstream of injection and the second figure shows how the flow is modified by the action of wall injection.

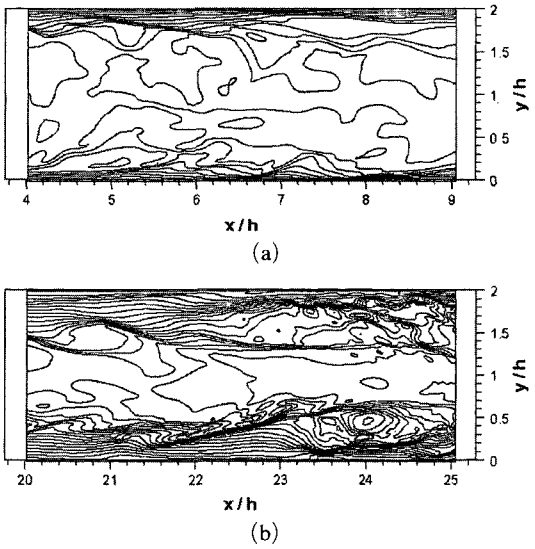

Fig. 2 Contours of streamwise velocity for Case-2 in the $(x-y)$ plane: (a) a region free from the influence of injection; (b) a region influenced by injection

Note that the wall-injection is applied from $x/h=13.4$. Mass conservation leads to a higher streamwise velocity in the middle of the channel as the flow moves downstream and locally, the wall blowing adds complexity to the flow as the boundary layer is displaced away from the wall and thus, it contains different flow elements including an outer flow and a free shear layer after $x/h=13.4$.

The progression of mean streamwise velocity profiles shown in Fig. 3(a)-(b) suggest that velocity profiles deviate significantly from that of non-transpired channel flow. At $x/h=15.1$ and 19.2, the log layer of the velocity profile appears to be disturbed significantly due to the wall blowing and this region falls below that of the regular velocity profile found in simple channel flow (say, velocity at $x/h=1.0$ or $x/h=9.1$). Thus, the 'law of the wall' does not hold at any streamwise locations after $x/h=13.4$ and the log layer of the velocity profile does not exist. This result may imply the presence of the larger length-scale which are formed in the shear layer (induced by the wall-injection) and this will be discussed further later (Fig. 9(b)). Since the boundary layer is displaced, the streamwise velocity gradient at the wall or equivalently a skin friction coefficient starts to decrease from $x/h=13.4$ until it recovers slowly after $x/h=20$ (Fig. 4).

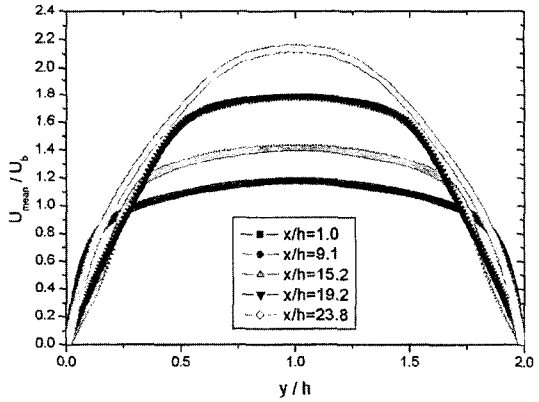

(a)

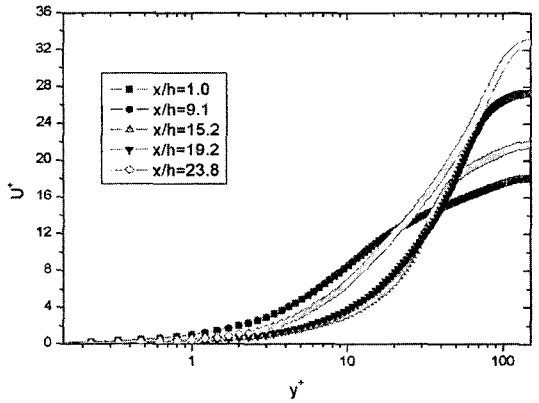

(b)

Fig. 3 Profiles of streamwise velocity at several streamwise locations for Case-2: (a) U_{mean} vs. y/h; (b) U^+ vs. y^+

Turbulent fluctuations and Reynolds shear stress for the Case-2 are shown in Figs. 5 and 6. Since the mean flow dynamics in the present injection-driven configuration are significantly different from those in non-transpired channel, the distributions of turbulence intensities and Reynolds shear stress show sizable departure as well. As the flow goes through a region of higher pressure gradient induced by the wall injection (compared to the smaller pressure gradient in the region $x/h<13$), Reynolds shear stress as well as turbulence intensities increases and it would be interesting to see the behavior of the Reynolds stress coefficient (i.e. normalized Reynolds shear stress), $R_{u'v'}=-\dfrac{\overline{u'v'}}{u_{rms}v_{rms}}$. Except for the location $x/h=15.1$ which is just downstream of the region where wall injection starts, the shape and the values do not change drastically compared to

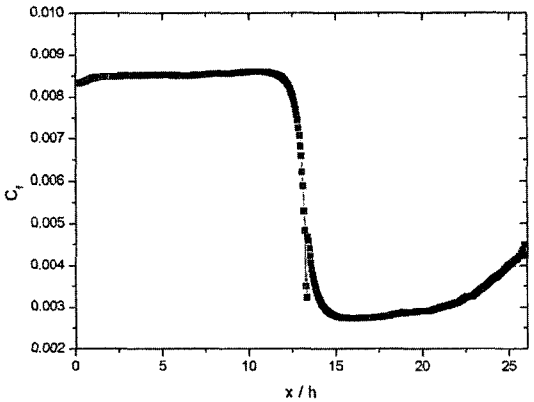

Fig. 4 Distribution of skin friction coefficient normalized by the inlet bulk velocity for Case-2

those upstream of injection (Fig. 7). Especially, the results for $x/h=19.2$ and 23.8 show that the coherence level of about 0.5 is maintained further away from the wall and this is attributed to the displacement of boundary layer upward by the action of wall blowing.

Figure 8 shows the turbulent viscosity at several streamwise locations. Significant variation of turbulent viscosity with x can be realizable and it is clear that the near-wall RANS modeling problem should be very different from that at non-transpired walls. At $x/h=15.1$, ν_t almost vanishes up to $y/h<0.125$ mainly due to the vanishingly small Reynolds shear stress at this location (Fig. 6). For $x/h>15.1$ turbulent viscosity increases abruptly as the flow moves downstream. Thus, the flow experiences very strong streamwise variations and it would not be an

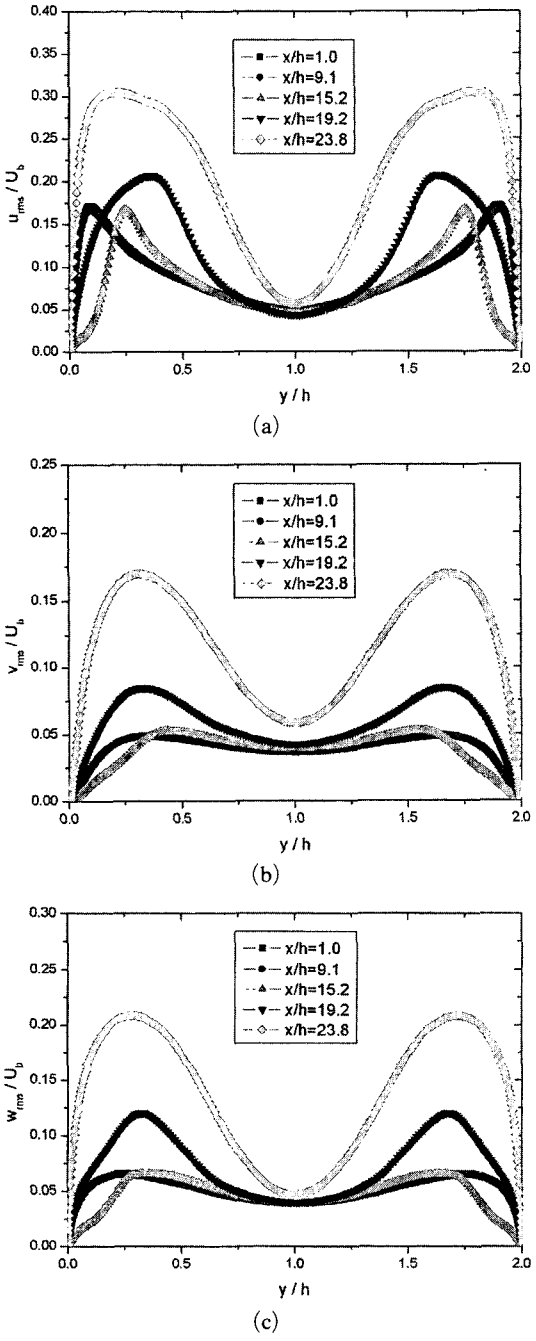

Fig. 5 Turbulence intensity profiles at several streamwise locations for Case-2: (a) u_{rms}; (b) v_{rms}; (c) w_{rms}

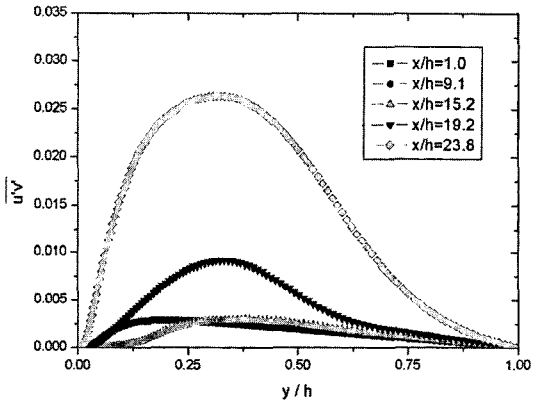

Fig. 6 Profiles of Reynolds shear stress at several streamwise locations for Case-2

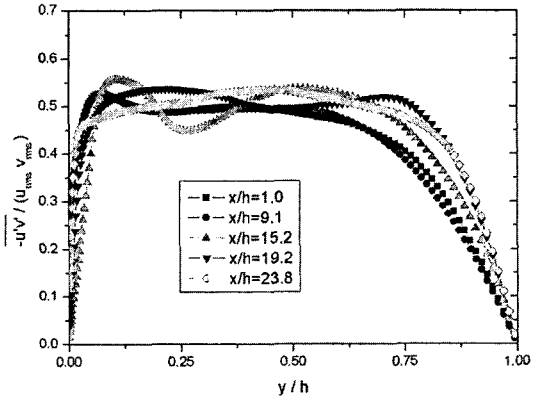

Fig. 7 Profiles of Reynolds shear stress coefficient for Case-2. $R_{u'v'}=-\dfrac{\overline{u'v'}}{u_{rms}v_{rms}}$

easy task to model the ν_t in this type of situation.

Fig. 9(a) shows the spanwise vorticity contours in the $(x\text{-}z)$ plane in the vicinity of the wall. It is seen that the streaks present in a non-transpiring channel flow are not present between $x/h=13.4$ and 22. Near-wall structures are totally displaced upward due to the strong wall blowing and subsequently different types of structures start to appear as the flow moves downstream. It is thought to be due to the shear instability induced by the interaction of the flow in the x-direction and the injected flow in the y-direction after the location where the wall blowing is applied. It is more clearly illustrated in Fig. 9(b) which shows the spanwise-averaged pressure fluctuations in an $(x-y)$ plane. This plot shows the difference in eddy length scales between the far upstream and the downstream of wall injection. The small scale structures grow rapidly in the shear layer and the resulting large 2-D like structures with alternating flow pattern (positive and then negative contours of pressure fluctuations) convect downstream. This is attributed to the passage of large vortical structures since the pressure is relatively low in the cores of vortices and it is relatively high between two cores. As discussed earlier in Fig 3(b), the persistence of the dip below the low-law implies the persistence of large structures which survive a long time before they break up into smaller, dissipative eddies.

Figure 10 shows the following mean momentum equation budget for streamwise velocity at $x/h=19.2$ for Case-2.

$$0=-\left(\frac{\partial\bar{u}\,\bar{u}}{\partial x}+\frac{\partial\bar{u}\,\bar{v}}{\partial y}\right)-\frac{\partial\bar{p}}{\partial x}+\frac{1}{Re_h}\left(\frac{\partial^2\bar{u}}{\partial x^2}+\frac{\partial^2\bar{u}}{\partial y^2}\right)-\left(\frac{\partial\overline{u'u'}}{\partial x}+\frac{\partial\overline{u'v'}}{\partial y}\right) \tag{4}$$

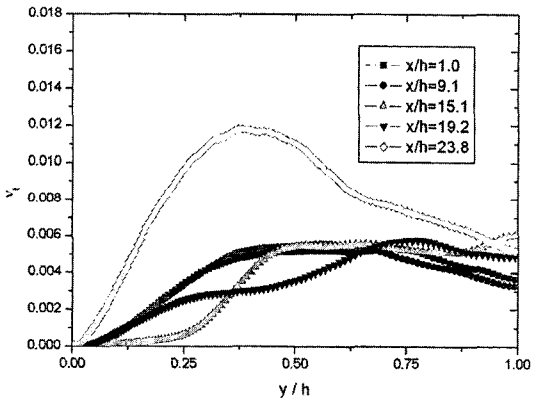

Fig. 8 Profiles of kinematic viscosity for Case-2

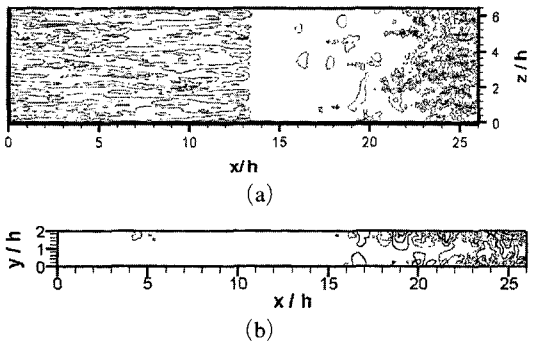

Fig. 9 (a) Contours of spanwise vorticity in the vicinity of the wall for Case-2.
solid line: positive contour values,
dotted line: negative contour values;
(b) Contours of spanwise averaged pressure fluctuations for Case-2.
solid line: positive contour values,
dotted line: negative contour values

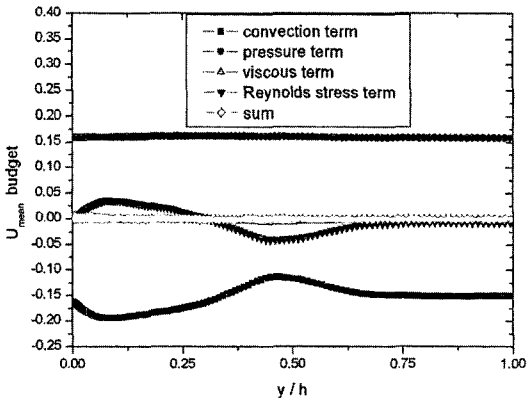

Fig. 10 Mean U-momentum equation budget for Case-2 at $x/h=19.2$.
convection term, $-\left(\frac{\partial\bar{u}\,\bar{u}}{\partial x}+\frac{\partial\bar{u}\,\bar{v}}{\partial y}\right)$
pressure term, $-\frac{\partial\bar{p}}{\partial x}$;
viscous term, $\frac{1}{Re_h}\left(\frac{\partial^2\bar{u}}{\partial x^2}+\frac{\partial^2\bar{u}}{\partial y^2}\right)$;
Reynolds stress term, $-\left(\frac{\partial\overline{u'u'}}{\partial x}+\frac{\partial\overline{u'v'}}{\partial y}\right)$

For non-transpired walls, the Reynolds stress and viscous terms are dominant very near the wall and usually the variation of terms in the streamwise direction is negligible compared to that in the wall normal direction. But Fig. 10 clearly reveals that the convection term i.e., a term related to streamwise acceleration and a pressure gradient term are dominant throughout the channel. The fact that the Reynolds term is an order of magnitude smaller than any other terms suggests that if one wants to predict the mean flow only, the results will not be very sensitive regardless of turbulence models used since the mean flow is not strongly influenced by the turbulence.

4. Summary

A model injection-driven internal flow has been investigated using a DNS technique to obtain detailed flow field information for turbulence modeling and LES development. It was shown that the mean flow dynamics and turbulence quantities differ significantly from those in typical non-transpired channel flows. This has important consequences for RANS type modeling because most of the turbulence models tuned for non-transpired walls are not expected to work equally well for the present flow.

The complexity of the flow comes from the interaction of the mean flow with strongly injected normal flow and the subsequent non-negligible streamwise inhomogeneity. This inhomogeneity would aggravate the performance of currently available models for subgrid-scale energy transfer and it would be interesting to see if widely-used standard LES strategy can deal with such inhomogeneities.

Spanwise vorticity contours show that the streak-like structures displaced away from the wall and the iso-surfaces of spanwise-averaged pressure fluctuations suggest that large structures grow in the shear layer and convect downstream. A frequency or time-scale of this motion was not measured in the present work but it is clear that the appearance of 2-D like structures will add to the difficulty of RANS type modeling work.

Acknowledgment

This research was supported by the Agency for Defense Development under the contract UD010006AD.

References

Beddini, R. A., 1986, "Injection-Induced Flows in Porous Walled Ducts," *AIAA J.*, Vol. 24, No. 11, pp. 1766~1773.

Dunlap, R., Blackner, A. M., Waugh, R. C., Brown, R. S. and Willoughby, P. G., 1990, "Internal Flow Field Studies in a Simulated Cylindrical Port Rocket Chamber," *J. Prop. Power*, Vol. 6, No. 6, pp. 690~704.

Harlow, F. H. and Welch, J. E., 1965, "Numerical Calculation of Time Dependent Viscous Incompressible Flow of Fluid with Free Surface," *Phys. Fluids*, Vol. 8, pp. 2182~2189.

Kasagi, N. and Shikazono, N., 1995, "Contribution of Direct Numerical Simulation to Understanding and Modeling Turbulent Transport," *Proc. R. Soc. Lond. A.*, Vol. 45, pp. 257~292.

Kim, J., Moin, P. and Moser, R., 1989, "Turbulence Statistics in Fully Developed Channel Flow at Low Reynolds Number," *J. Fluid Mech.*, Vol. 177, pp. 133~166.

Liou, T. M. and Lien, W. Y., 1995, "Numerical Simulations of Injection-Driven Flows in a Two Dimensional Nozzleless Solid Rocket Motor," *J. Prop. Power*, Vol. 11, No. 4, pp. 600~606.

Lund, T., Wu, X. and Squires, K., 1998, "Generation of Turbulent Inflow Data for Spatially Developing Boundary Layer Simulation," *J. Comput. Physics*, Vol. 140, pp. 233~258.

Miyauchi, T. and Tanahashi, M., 1993, "Test case : Temporally Developing Chemically Reacting Turbulent Mixing Layer," http://www.thtlab.t.u-tokyo.ac.jp.

Na, Y., Papavassiliou, D. V. and Hanratty, T., 1999, "Use of Direct Numerical Simulation to Study the Effect of Prandtl Number on Temperature Fields," *Int. J. Heat and Fluid Flow*, Vol. 20, pp. 187~195.

Spalart, P. R., Moser, R. D. and Rogers, M., 1991, "Spectral Methods for the Navier-Stokes Equations with One Infinite and Two Periodic Directions," *J. Comput. Phys.*, Vol. 96, pp. 297~324.

Traineau, J. -C., Hervat, P. and Kuentzmann, P., 1986, "Cold Flow Simulations of a Two Dimensional Nozzleless Rocket Motor," Tech. Rep. 86-1447. AIAA.

Williams, F. A., Barrere, M. and Huang, N. C. 1969, "Fundamental Aspects of Solid Propellant Rockets," NATO AGARDograph, No. 16.